

# A98-31490

ICAS-98-2,1,2

## ONERA ACTIVITIES ON SUPERSONIC TRANSPORT AIRCRAFT AERODYNAMICS

J.J. Thibert, Ph. Duveau, R. Grenon, P. Lemée, R. Thépot

Office National d'Etudes et de Recherches Aérospatiales  
Châtillon, France

### Abstract

During these last few years ONERA activities on supersonic transport aircraft aerodynamics have been oriented towards CFD code assessment for performance prediction and in particular for the drag, the development of numerical optimisation tools for multipoint designs, drag reduction technology investigations and air intake aerodynamics.

Euler and boundary layer codes are able to predict the general features of the flow for all the flight conditions. Accuracy of the drag prediction is satisfactory in supersonic but not so good in transonic. At low speed and high angle of attack Euler solutions suffer from too much artificial dissipation.

Numerical optimisation techniques are able to deal with a great number of design variables and are powerful tools for multipoint designs. Several design exercises have demonstrated the capabilities of this method to significantly improve current designs.

Drag reduction technologies can also be foreseen for application on a supersonic transport aircraft. In particular riblets are efficient for reducing the skin friction drag. Laminar flow control is not very powerful with the actual wing shapes and would need specific design as well as efficient systems to avoid leading edge contamination.

CFD tools are also able to predict correctly air intake performances near adaptation but they have still to demonstrate their capacities for off-design situations as well as for the internal shock control system design.

### Introduction

ONERA has been involved for several years in close cooperation with Aerospatiale and SNECMA in research concerning the future supersonic transport aircraft (SCT). This research programme which is supported by the French governmental agencies (DGAC, STPA) aims at the development of tools, methodologies, and technologies to be used for this new aircraft. ONERA activities concern propulsion, structures, environment, noise and aerodynamics.

This paper give a short overview if the ONERA activities in the aerodynamic field.

Pre-design studies carried out by the European manufacturers indicate that this new aircraft will probably have the main characteristics shown in **figure 1**. The weight breakdown for a typical range of 5 500 nm given in **figure 2** shows that the payload represents about 8 % of the gross weight while it is about 20 % for a subsonic long range aircraft.

- \* PASSENGERS : 250\* (3 classes)
- \* RANGE : • 5500 nm. (at entry into service)  
• 6500 nm. (later version at higher T.O. weight)
- \* CRUISE SPEED : • SUPERSONIC : MACH 2.05  
• SUBSONIC : M = 0.95
- \* CRUISE ALTITUDE : 50 000 < Z < 65 000 ft
- \* ENVIRONMENT : • POLLUTION : minimum NO<sub>x</sub> injection near ozone layer to be defined  
• NOISE : FAR 36, stage 3 regulation around airports  
• SONIC BOOM : no supersonic flight over inhabited area

FIGURE 1 - Future SCT Aircraft - Main characteristics

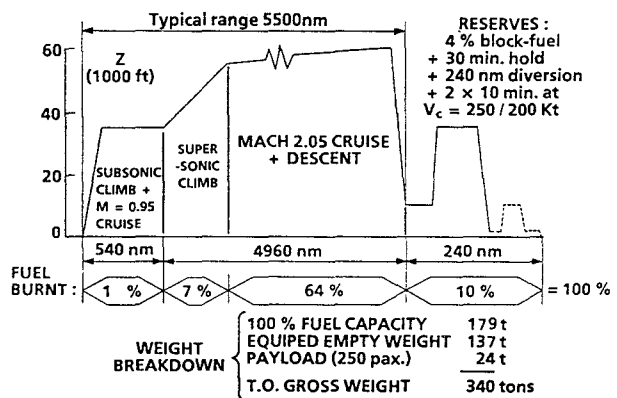


FIGURE 2 - Weight breakdown for a 5 500 nm trip

The fuel part in the D.O.C. will probably be around 35 % while it is only 27 % for a subsonic aircraft. The relatively low payload and the high part of

the fuel in the D.O.C. make this aircraft very sensitive to the aerodynamic performances. Compared to Concorde this aircraft will be bigger as shown in **figure 3** with about a double span and an aspect ratio around 2. The wing planform is chosen to provide high L/D at supersonic and transonic speeds and the expected gains compared to Concorde are about 40 %. Thus the drag is the key issue for this aircraft. This is why the aerodynamic research activities at ONERA have been oriented to this main topic. They cover the following topics : prediction tools assessment and investigation of drag reduction technologies, advanced design tools development and air intake aerodynamics.

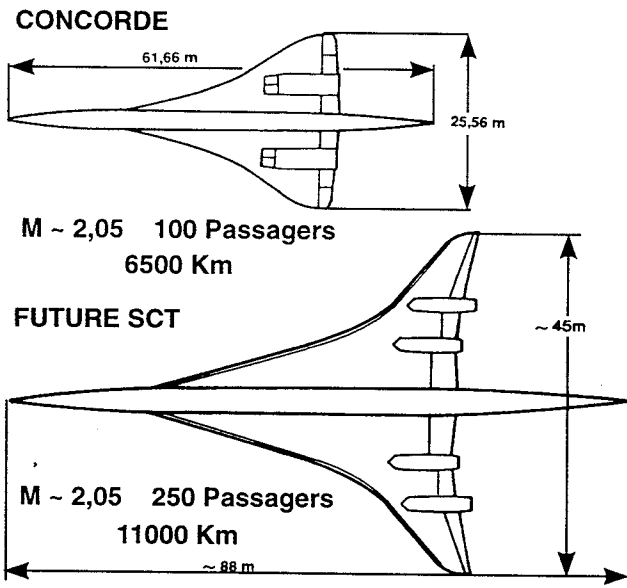


FIGURE 3 - Concorde and future SCT aircraft - Size comparison

Performance prediction

The aerodynamics of Concorde was based on approximate theoretical methods and intensive wind tunnel tests. CFD will play a much larger role for the next SCT aircraft since Navier Stokes, Euler codes and boundary layer codes are in principle able to predict the performances for all the flight conditions. However these tools have to be carefully assessed in order to determine their accuracy.

ONERA has developed these last years 2 main finite volume Euler/Navier Stokes codes, one for transonic and low supersonic speed flows (CANARI code) based on a centred scheme, the second one for supersonic and hypersonic flows (FLU3M code) based on an upwind scheme. The last one will be described later in the paper. The first solver <sup>(1)</sup> uses multidomain structured grids with potential overlapping. Time integration is the explicit multistage Runge Kutta, accelerated by the Lerat-Sides implicit method <sup>(2)</sup>.

Dissipative terms are the blended 2<sup>nd</sup> and 4<sup>th</sup> differences of Jameson and al <sup>(3)</sup>. Boundary conditions are based on the characteristic relations and various turbulence models are available.

This code has been used to compute the Aerospatiale ASTF configuration (wing + fuselage + fairings + fin) which was tested in the ONERA S2MA transonic + supersonic wind tunnel. Computations have been carried out on a grid of 1.2 million mesh points generated with the ICEM-CFD system. The Euler option (inviscid flow) was used and boundary layer computations were done without coupling with the 3C3D code <sup>(4)</sup> developed at ONERA-CERT.

Supersonic cruise Mach number

**Figure 4** presents the comparisons at Mach 2. The lift (**figure 4a**) and the drag (**figure 4b**) are well predicted as well as the pressure distribution (**figure 4c**). The computed pressure + friction drag is lower by about 5 counts than the experimental drag. As shown in **figure 4c** the outer wing leading edge is supersonic while the inner wing leading edge is subsonic due to the sweep angles.

FIGURE 4 - Performance prediction at Mach 2

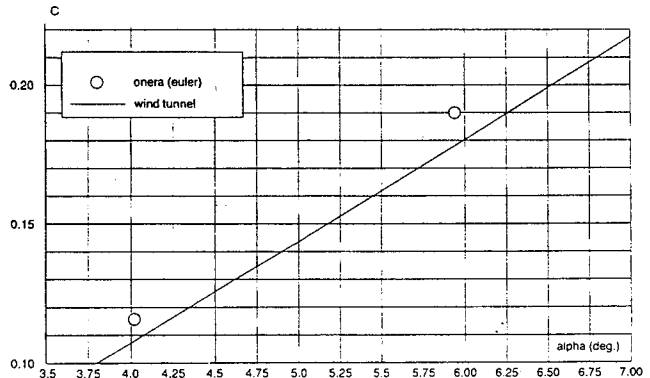


FIGURE 4a - Lift

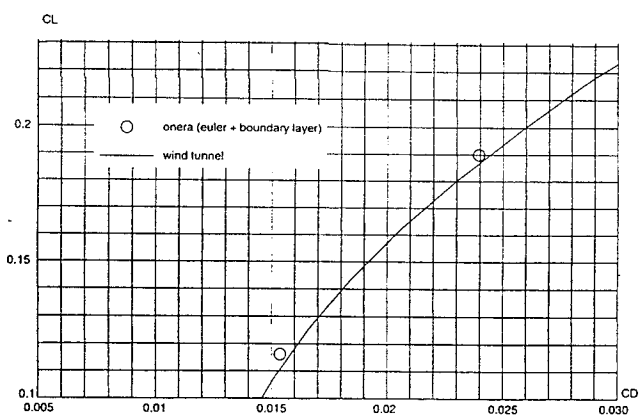


FIGURE 4b - Drag

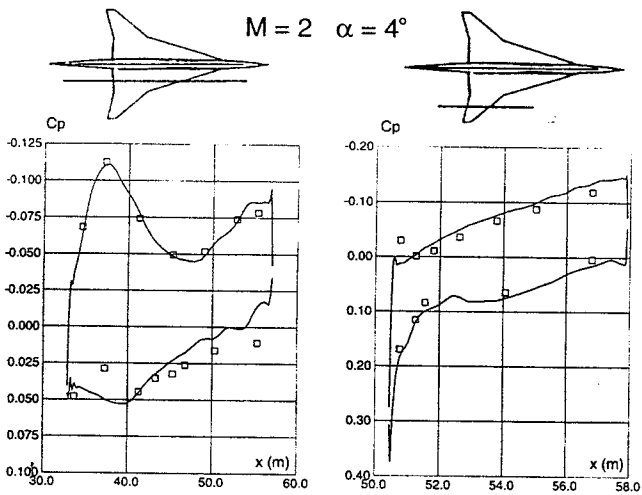
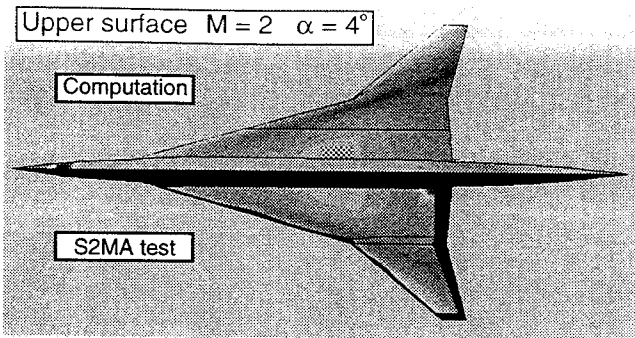


FIGURE 4c - Pressure distribution

Transonic cruise Mach number

The same comparisons are presented in **figure 5** for the transonic cruise Mach number 0.95. The lift is a little bit over-predicted by the inviscid computations (**figure 5a**). The computation gives the main feature of the flow (**figure 5c**) but the rear compression is sharper and closer to the trailing edge than in the experiment. Upstream of this compression, Euler solution shows supersonic flow expansion on the outer wing contrary to experiment.

The computed pressure + friction drag under-predicts the drag by about 20 counts which shows that for this Mach number coupled methods or NS methods are needed to better predict the drag.

FIGURE 5 - Performance prediction at Mach 0.95

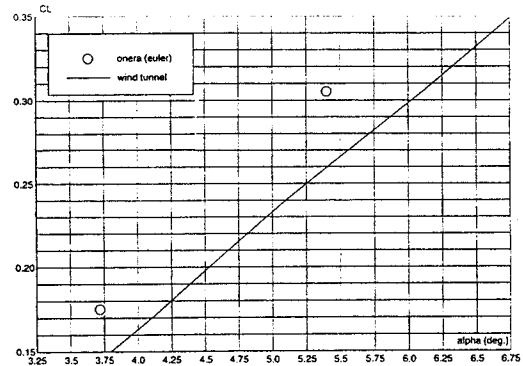


FIGURE 5a - Lift

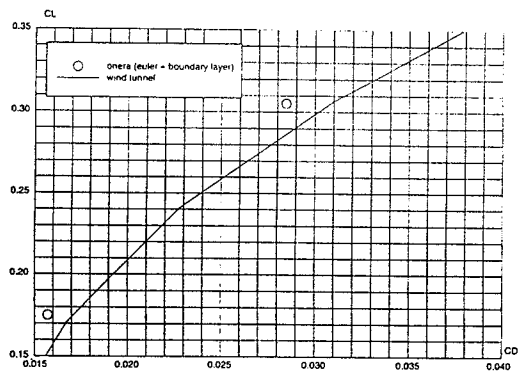


FIGURE 5b - Drag

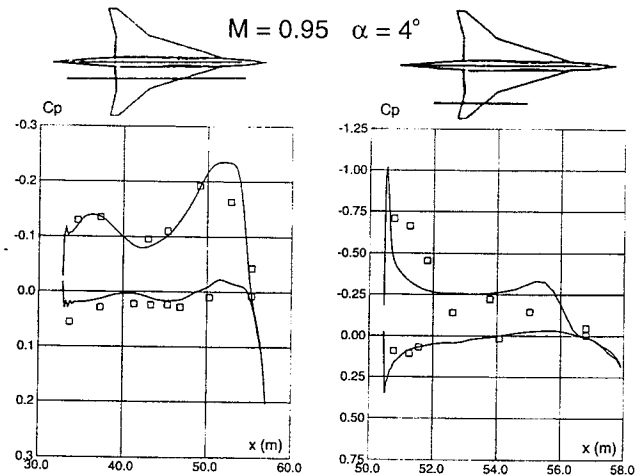
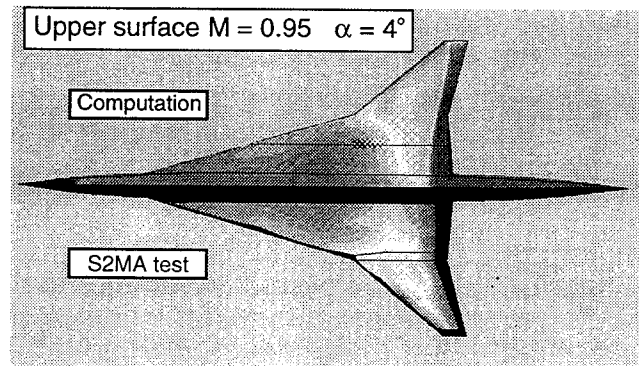


FIGURE 5c - Pressure distribution

Low speed

At low speed (Mach 0.25) and high angle of attack **figure 6a** shows that the flow is very complex with three vortices interacting on each other. The lift and the drag are underpredicted (**figure 6b and 6c**) but the difference remains about the same with the angle of attack which means that viscous effects are constant, the flow being separated on the upper surface. The pressure distribution is also correctly predicted [**figure 6d**] with a slight delay in the apex vortex formation. In order to complement the comparisons between Euler computations and experimental data at low speed and high angle of attack, other experiments have been performed on the same model in the S2 Chalais-Meudon low speed wind tunnel with LDV flow field measurements. The three components of the velocity have been measured in three planes above the wing (**figure 7a**).

FIGURE 6 - Performance prediction at Mach 0.25

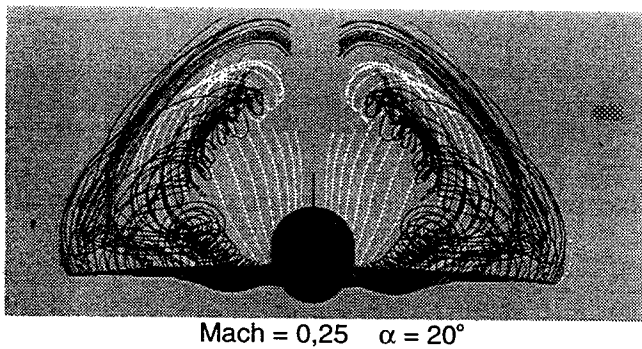


FIGURE 6a - Flow structure computed with the Euler code

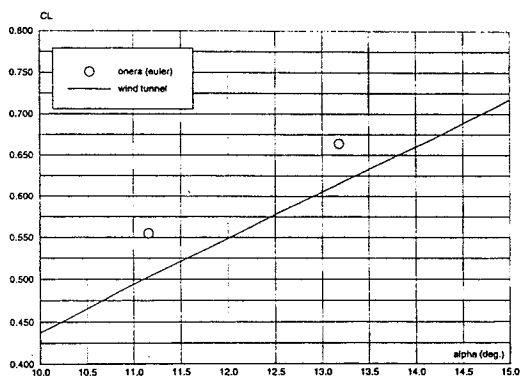


FIGURE 6b - Lift

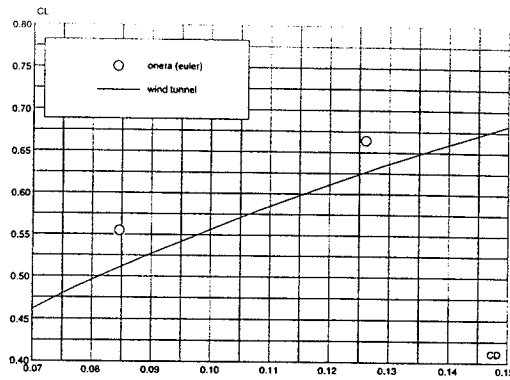


FIGURE 6c - Drag

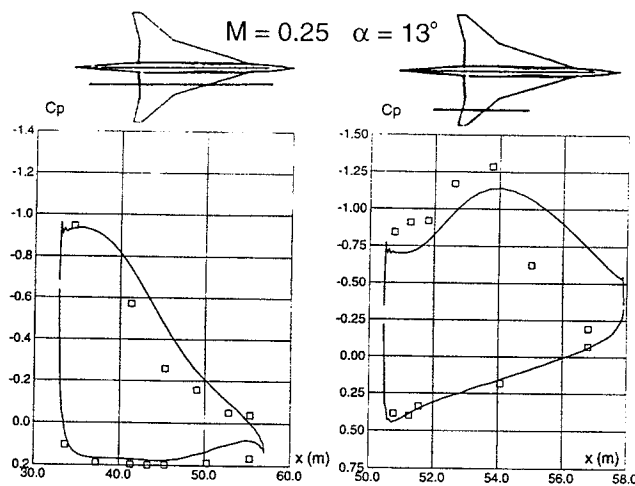


FIGURE 6d - Pressure distribution

FIGURE 7 - Vortex flow prediction at Mach 0.25

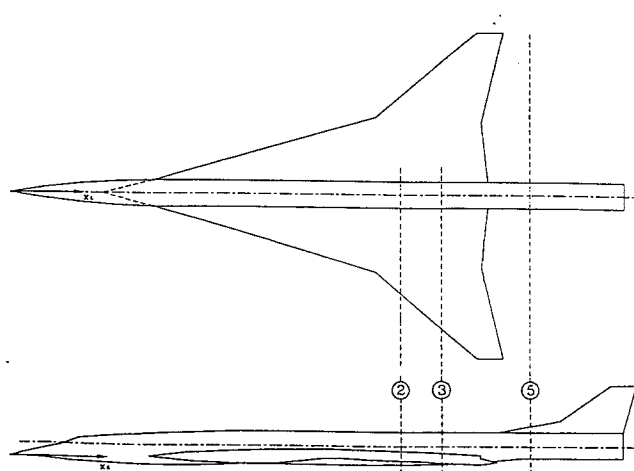


FIGURE 7a - Location of the measurement planes

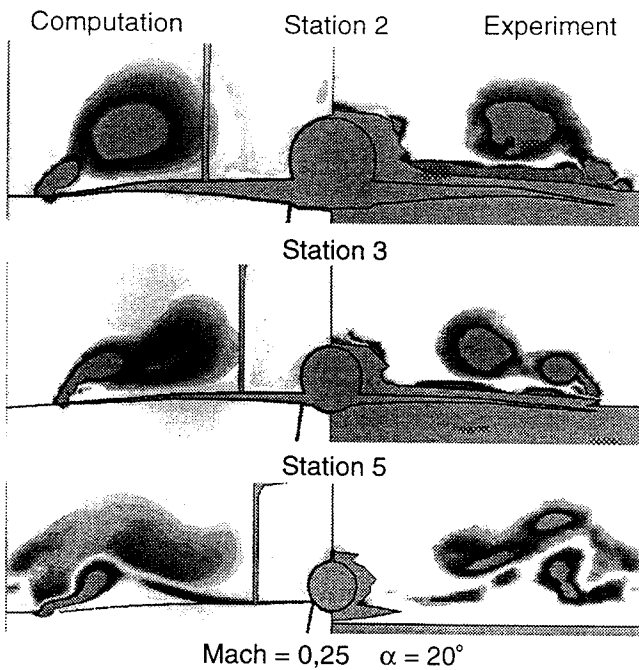


FIGURE 7b - Axial vorticity distribution

The axial vorticity distributions computed and measured in these three planes are compared in figure 7b for an angle of attack of 20°. In the first plane, the two vortices coming from the apex and the leading edge crank are well predicted. Downstream, for station 2, the inner vortex is more diffuse in the computation than in the experiment. Behind the trailing edge, at station 3, the computed vortices are completely diffused while there are still visible in the experiment. For this station the tip vortex is hardly visible both for experiment and for computation.

Wind tunnel/Flight extrapolation

Figure 8 presents the drag breakdown at Mach 2 for the cruise lift level. In wind tunnel conditions ( $Re \sim 13 \times 10^6$ ) the friction drag is about 43 % of the total drag. Reynolds number correction applied to the friction drag to extrapolate the drag to flight conditions ( $Re \sim 160 \times 10^6$ ) reduces drastically the drag. On the figure the full payload as well as 1 ton of payload have been expressed in term of drag to point out that the drag correction from wind tunnel to flight is higher than the full payload. This illustrates the degree of accuracy needed for wind tunnel data and for Reynolds number corrections because errors mean questionable predicted payload/range. Accurate Reynolds number correction implies reliable skin friction laws for high Reynolds numbers, this is why flight test measurements have been performed on a Concorde aircraft in order to measure the local skin friction. These measurements were carried out by Aerospatiale and ONERA/CERT<sup>(5)</sup>. Six measuring blocks were installed on

the aircraft, each one consisting of two pitot probes, one static probe and one thermocouple to measure the wall temperature as shown in figure 9. A calibration of these measuring blocks allows the incompressible skin friction coefficient to be determined from the measurements. The results plotted in figure 9 are in good agreement with the skin friction law proposed by Michel.

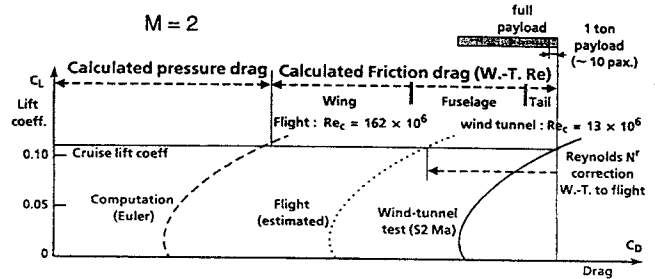


FIGURE 8 - Drag breakdown at Mach 2

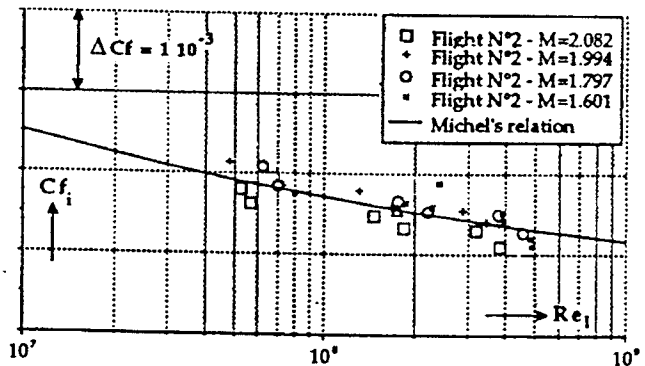
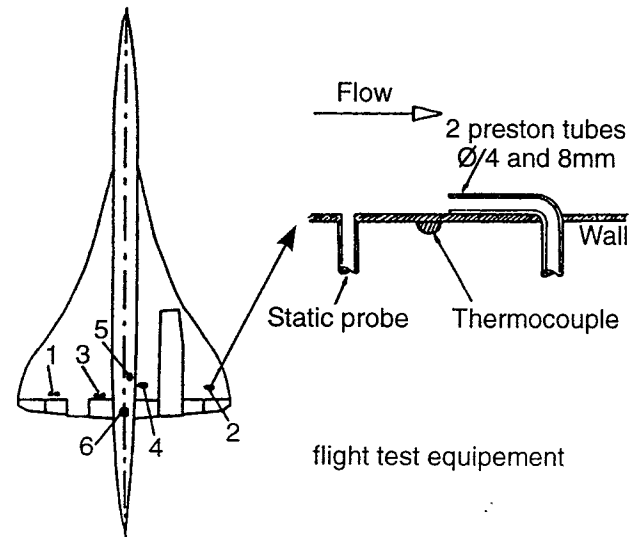


FIGURE 9 - Concorde flight test - Skin friction data

Wing design by numerical optimisation

The future SCT aircraft will probably fly overland at transonic speed. Thus its design will be a compromise between supersonic and transonic performances. Numerical optimisation techniques are powerful tools for this kind of multipoint designs.

They have been used at ONERA for several years to improve airfoil and wing designs at transonic speed <sup>(6) (7)</sup>. For these applications the number of design variables was rather low and the aerodynamic computations were performed with potential codes.

Three years ago the method was extended to allow wing-body configuration optimisation with Euler codes and to deal with a great number of design variables. The general organisation of the ONERA optimisation code is described in figure 10. The code is built around the CONMIN and COPES codes <sup>(8) (9)</sup> with :

- a geometry generator which modifies the wing-body geometry,
- a geometric constraints module,
- a grid generator,
- an Euler code.

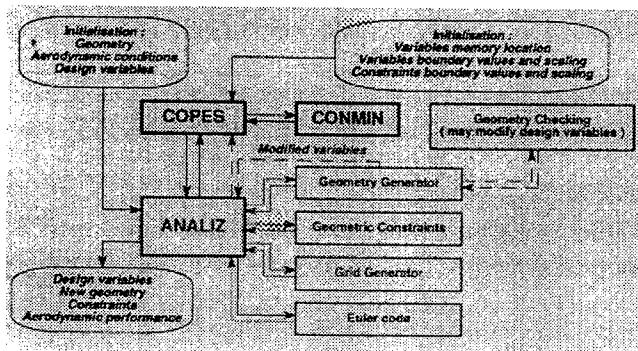


FIGURE 10 - Structure of the ONERA optimisation code

All these routines are controlled by the ANALYZ routine which ensure the interfaces. More details about this code can be found in <sup>(10)</sup>. Bezier curves are used for wing twist, camber and thickness modifications and specific modules have been built for wing planform and wing location controls. The grid generator builds O type grids around wings and wing-body configurations using simple algebraic methods. Typical mesh sizes are about 30 000 cells and the Euler code is the one described before.

The code has been applied to the optimisation of the ATSF configuration. The objective was to reduce the inviscid drag by modifying the twist and the camber laws. Three optimisations were performed starting with the same

initial shape :

- single point optimisation at Mach 2,
- single point optimisation at Mach 0.95,
- dual point optimisation.

For each case 25 design variables were used and about 20 cycles were needed for each optimisation. The three optimised wings have been computed in a fine grid in order to improve the drag prediction accuracy. In figure 11a the performances of the initial wing and of the optimised ones are compared at Mach 2 and for an angle of attack of 4° (supersonic cruise conditions). The supersonic single point optimisation reduces the drag of the ATSF wing by 4 per cent, the transonic optimisation by 3.2 per cent and the dual points optimisation by 2.5 per cent. The lift cannot be maintained during the transonic optimisation for the given angle of attack. The pressure distributions show that the supersonic optimisation decreases the maximum velocity on the upper surface mainly on the trailing part of the low pressure area which follows the highly swept leading edge. The transonic design reduces too much the load at the leading edge of the outer wing while the two points design seems to be in between the two single points designs. The performances for the transonic cruise point (Mach 0.95  $\alpha=4^\circ$ ) are presented in figure 11b. The drag reduction is 5.4 per cent for the supersonic design, 17.5 per cent for the transonic design and 9.8% for the two points design. The lift is kept approximately constant for this case. Pressure distributions show that while the supersonic design has a small effect, the transonic design eliminates almost completely the velocity peak along the leading edge mainly on the outer part of the wing but increases slightly the Mach number before the shock. For the two points design pressure distributions are in between those given by the two single point optimisations.

FIGURE 11 - One point and two points optimisation of the ATSF wing

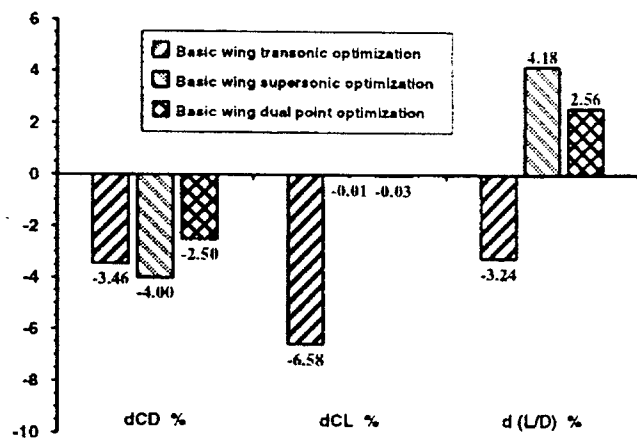


FIGURE 11a - Performance comparison at M=2,  $\alpha=4^\circ$

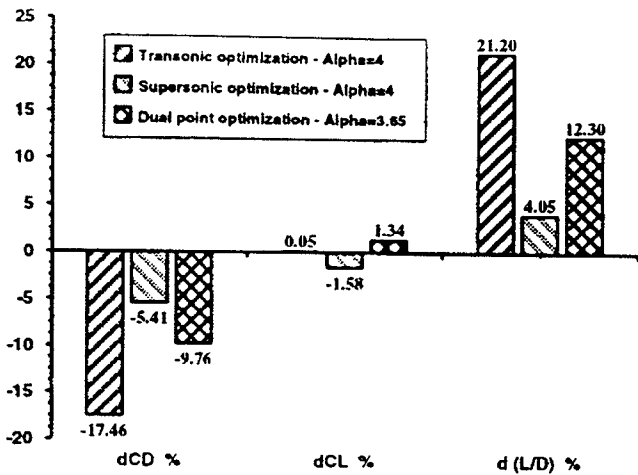


FIGURE 11b - Performance comparison at  $M=0.95$ ,  $\alpha=4^\circ$

Another optimisation exercise has been performed on the configuration called European Supersonic Civil Transport (ESCT) shown in figure 12. For that case the slat leading edge deflections were determined in order to optimise the L/D for the transonic cruise point. The control surfaces are shown in figure 12. The leading edge of the wing has been split in three parts on which different deflections can be applied. The optimisation computes the best combination of the slats together with the value of the angle of attack, the lift being constrained to a value of 0.2. Since the computations are made in inviscid flow, some constraints were also put on the pressure coefficient at the hinge to avoid too large an expansion. Sixty cycles were needed to obtain a good solution. The L/D is increased by 14.8 per cent with the slat deflections given in figure 12. The leading edge droop reduces the velocity in that region but increases the velocity slightly ahead of the rear shock.

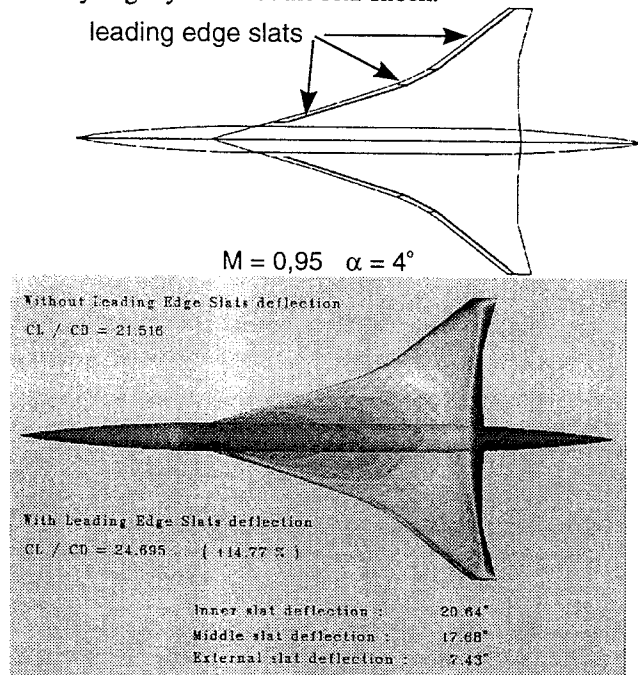


FIGURE 12 - Leading edge slats deflections optimisation ESCT configuration  $M=0.95$ ,  $\alpha=4^\circ$

These examples show that significant improvements of the L/D can be obtained through the use of numerical optimisation. Multipoint capabilities as well as the possibility to deal with geometrical constraints make this type of method very attractive for such design even if the computing time is quite large.

### Drag reduction technologies

Since ONERA has been involved for some years in research aiming at the drag reduction of subsonic aircraft <sup>(11)</sup> <sup>(12)</sup> it seems worthwhile to investigate the potential drag benefit for supersonic transport aircraft by using these techniques.

### Turbulent skin friction drag reduction

Riblets have proven to be efficient in the reduction of the turbulent skin friction drag in wind tunnel and in flight <sup>(13)</sup>. They have also been tested in supersonic flow on a simplified cone-cylinder model <sup>(14)</sup> for Mach numbers between 1.6 and 2.5 and Reynolds numbers ranging from 5.5 to 22.5 million per meter (figure 13). Different sizes of "V grooved" shapes provided by the 3M company were glued on the cylindrical part of the model. A maximum of 6 per cent of skin friction drag reduction has been measured for a height of the riblets expressed with the wall variables of about 10. This is slightly lower than in subsonic flow but it can provide for the complete aircraft a total drag reduction between 1 and 2 per cent depending on the surface area on which riblets are applied.

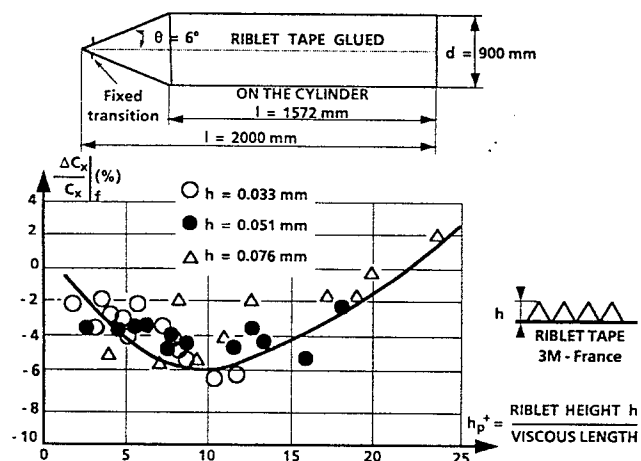


FIGURE 13 - Skin friction drag reduction with riblets in supersonic flow

### Laminar flow control

The configuration chosen for the evaluation of drag reduction through laminar flow control is the ESCT presented in the previous section. The study was done for the supersonic cruise condition (Mach = 2).

Euler computations were first made on the wing body geometry (figure 14a). Special attention has been paid for the mesh near the leading edge in order to compute accurately the pressure distribution as shown in figure 14b for a section located at 30 per cent of the span.

FIGURE 14 - ESCT configuration  $M=2$ ,  $\alpha=4^\circ$

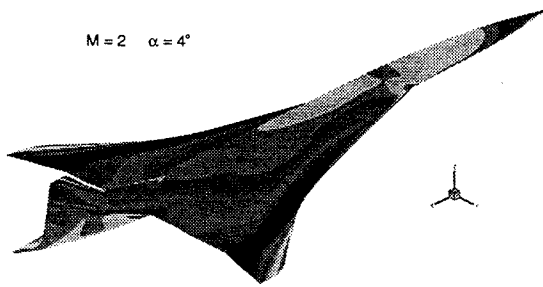


FIGURE 14a - Computed pressure distribution

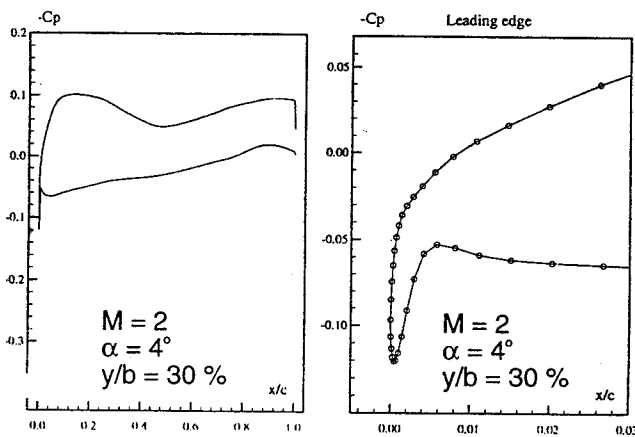


FIGURE 14b - Pressure distribution for the 30 % span section

Boundary layer computations were then performed and the transition location was predicted with a data base method<sup>(15)</sup> for TS instabilities and with a semi empirical criteria<sup>(16)</sup> for the cross flow instabilities. These predictions were checked with linear stability computations<sup>(17)</sup> for some cases. Figure 15a shows that for a constant suction applied between 0 and 20 % of the chord it is possible to move the transition downstream up to 30 % of the chord in the inner part of the wing. This figure shows also that the simple criteria are in good agreement with the stability computations for predicting the transition location. The next step consisted in the optimisation of the suction distribution both in the streamwise and in the spanwise directions in order to minimise the sucked mass flow rate. With five independent suction chambers along the leading edge, through which different suction velocities can be applied, it is possible to achieve higher drag reduction than

by keeping the same suction velocity all over the span. This arrangement allows the suction mass flow to be largely reduced as shown in figure 15b. The transition location on the upper surface ranges from 25 % of the chord near the wing root to 60 % of the chord at the tip. The total aircraft drag reduction has been estimated at about 4 % with a suction mass flow of 6 kg/s. Taking into account the power needed for the suction the fuel consumption reduction is about 3 %.

FIGURE 15 - ESCT configuration - Wing laminarization at  $M=2$

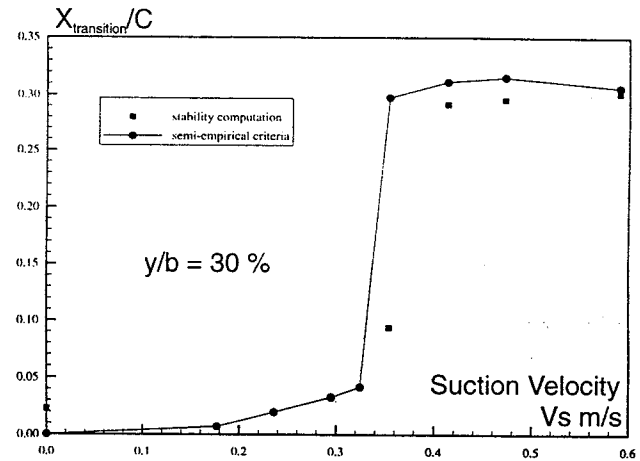


FIGURE 15a - Transition location versus Velocity

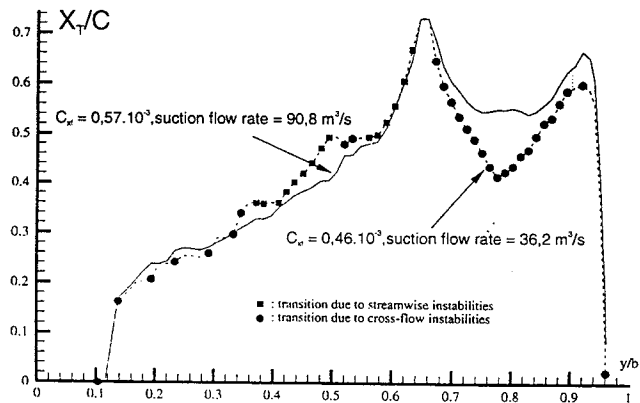


FIGURE 15b - Transition location on the wing upper surface

This study shows that with a turbulent wing design potential gains by applying laminar flow control are relatively low. They probably can be increased significantly through the optimisation of the pressure distribution and this is being investigated at the moment.

Anyhow the application of Laminar Flow Control on Supersonic aircraft will raise difficult technical problems due to the small thickness of the wing.



Leading edge contamination

In order to apply Laminar Flow Control the attachment line on the wing has to be laminar. Several solutions have been successfully tested for transonic swept wings at ONERA <sup>(18)</sup> but no experience exists for supersonic wings. This is why as a first step two experiments have been performed in order to investigate leading edge flows on swept wings in supersonic flow. The main objective was to assess the criteria proposed by Poll for leading edge contamination.

The first experiment <sup>(19)</sup> was carried out on a cylinder placed with a sweep angle in the jet exhaust of the supersonic R1 Chalais-Meudon wind tunnel. The experimental data showed that leading edge contamination occurs for  $\bar{R}^* \geq 250$ .

FIGURE 16 - Leading edge contamination

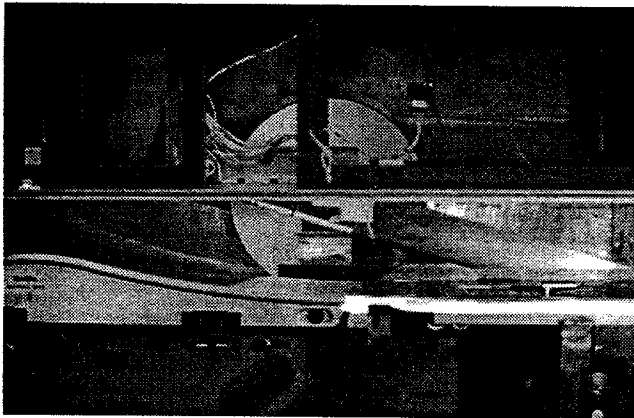


FIGURE 16a - Test set up

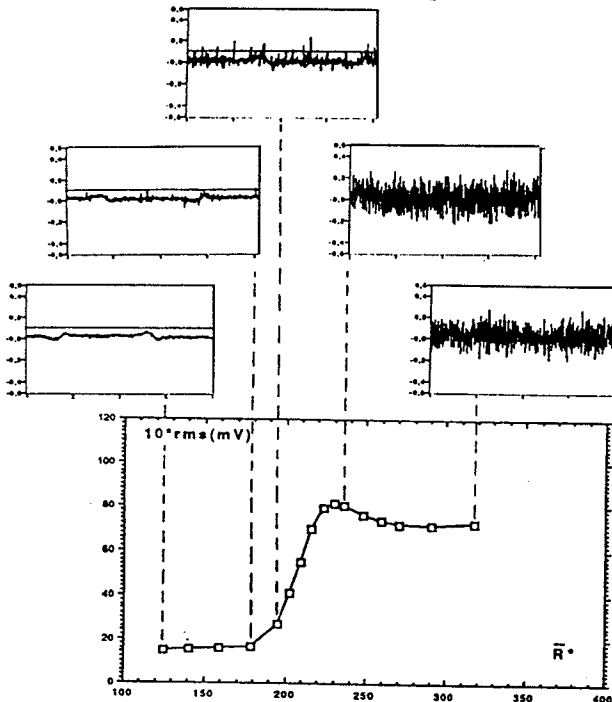


FIGURE 16b - Leading edge hot film signals

This value has also been confirmed by another experiment on a swept wing whose leading edge was designed to provide in the wind tunnel conditions  $\bar{R}^*$  values close to the flight values. The wing was tested in the supersonic S5 Chalais-Meudon wind tunnel for Mach numbers 2 and 2.5 (figure 16a). Pressure distribution around the leading edge and wall temperature measurements allow to compute  $\bar{R}^*$ . The state of the boundary layer is determined through hot films signals as shown in figure 16b. For  $\bar{R}^*$  values  $< 200$  signals indicate a laminar boundary layer. For  $\bar{R}^* \sim 200$  turbulent spots appear and for  $\bar{R}^* > 250$  the signals show that the boundary layer is turbulent.

These studies are being pursued in order to investigate various passive devices which could avoid leading edge contamination.

Air intake aerodynamics

Another major issue for the next supersonic transport aircraft is the air intake performance since a one per cent loss in the pressure recovery at Mach 2 would give a penalty of two per cent for the payload.

Concorde air intakes were optimised through intensive wind tunnel testing. These air intakes exhibit very good performances in terms of efficiency, stability and control. For the future SCT the objective is to have the same performances together with a reduction of the cowl drag. This can be achieved by increasing the internal compression compared to the Concorde air intake, the counter part being a reduction of the margin between the adaptation and off design problems like unstart phenomena <sup>(20) (21)</sup>. Thus an advanced control system will be needed if a mixed compression air intake is chosen.

The inlet has also to be adjustable to meet the requirements under many different flight conditions, from take off to supersonic cruise. The design is also constrained by the auxiliary doors needed to increase the engine mass flow at subsonic speed and by the type of nozzle which will be retained.

Activities at ONERA concerning air intakes aerodynamic are oriented toward CFD code assessment for the performance prediction and basic research aiming at a better understanding of the complex flow inside the air intake in order to design an efficient and reliable control system.

Air intake performance prediction

The two ONERA Euler/Navier Stokes codes developed at ONERA are currently used for air intakes aerodynamic studies. The first one (CANARI code) which uses a centred scheme has already been described in a previous section of the paper. The second one (FLU3M code) is a finite volume, cell centred code which uses an upwind scheme with MUSCL extrapolation and has a second order accuracy in space on regular meshes <sup>(22)</sup>. Van Leer, minmod and other limiters are available in order to satisfy Total Variation Diminishing condition. For viscous calculations, Roe's scheme is used together with Harten correction and minmod limiter. An ADI factorisation technique is applied for implicit time stepping.

A generic 2D simple compression ramp air intake model shown in **figure 17a** has been used for parametric studies in the S3 Modane supersonic blow down wind tunnel. Experimental data include wall static pressure distribution, and detailed pitot probings at various locations.

These data have been used to assess the Euler/Navier Stokes codes. 3D inviscid FLU3M computations were performed at Mach 2 for different operating conditions. **Figure 17b** shows that the computational results exhibit flow features which are close to the ones given by the schlieren picture for the critical regime.

2D Navier Stokes computations with the Jones-Lauder k-ε turbulence model are presented in **figure 17c**. The pressure recovery is quite well predicted with both codes but the mass flow is over predicted due to the lateral flow spillage which is not accounted for in these 2D computations. The total pressure profiles plotted in **figure 17d** show that the codes predict the pressure profile quite well at the end of the diffuser.

FIGURE 17 - Schematic 2D air intake. Computer codes assesment

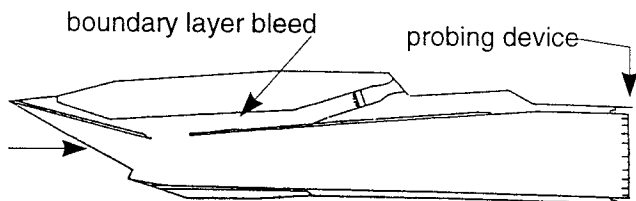


FIGURE 17a - Wind tunnel model

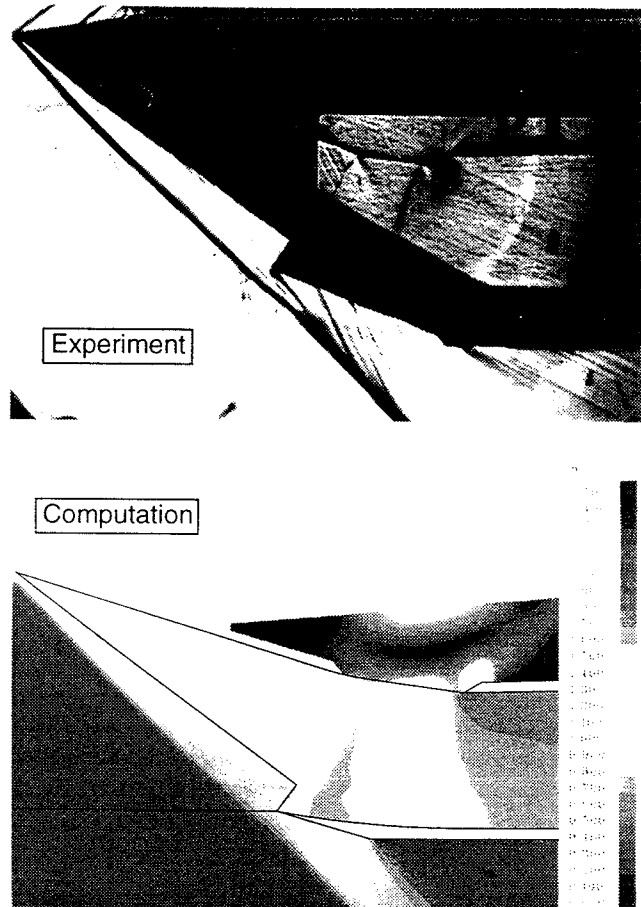


FIGURE 17b - Flow field comparison for the critical condition

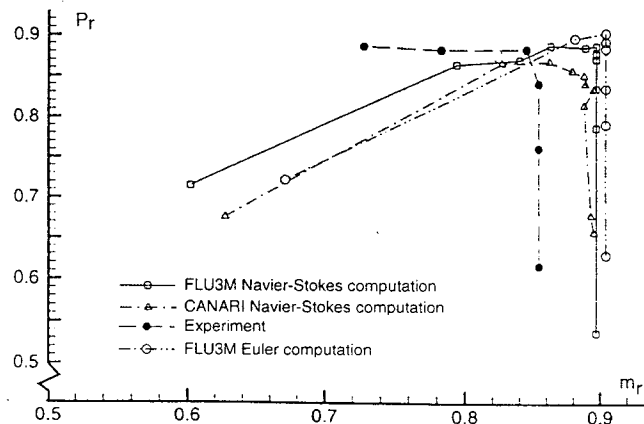


FIGURE 17c - Air intake performance prediction

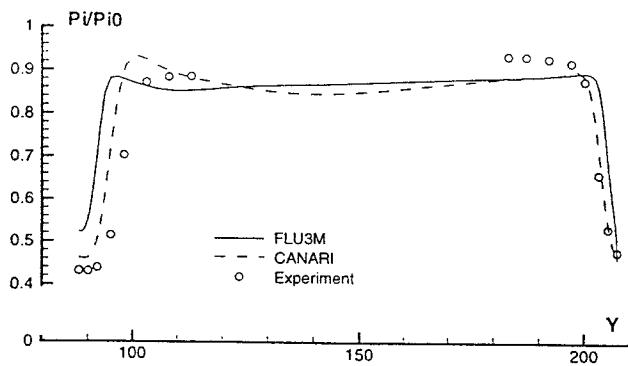


FIGURE 17d - Prediction of the total pressure profiles at the end of the diffuser

For a cruise Mach number of 2.4 which is also being investigated by the manufacturers, axisymmetric air intakes provide some advantages compared to 2D geometries. For this Mach number mixed compression air intakes are needed in order to avoid too large a cowl drag. Such an air intake, designed by Aerospatiale, has been computed with the FLU3M code and the results are presented in figure 18. The flow field for the critical regime shows that the supersonic compression is achieved both by the centerbody and the internal cowl, the subsonic compression taking place inside the diffuse downstream of the inlet throat. The operating characteristic curves obtained from Euler and Navier Stokes computations are plotted in figure 18. Both calculations indicate that there is no stability margin as expected for this type of air intake. The maximum pressure recovery predicted by Navier Stokes calculations is clearly lower than the inviscid value because the unstart of the inlet occurs earlier in viscous flow. An increase of the bleed flow would likely increase the efficiency computed in viscous flow.

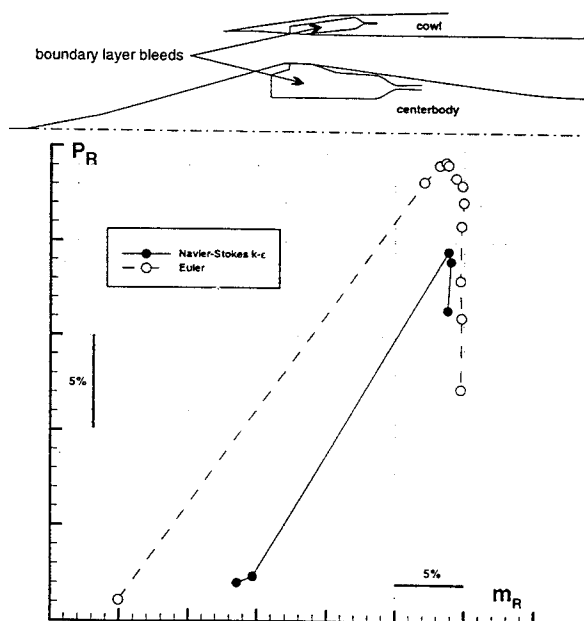


FIGURE 18 - Axisymmetric mixed compression air intake. Performance prediction at  $M=2.4$

#### Air intake shock control

Mixed compression air intakes need a control system to provide sufficient margins between the design operating conditions and the unstart of the inlet. This will probably be achieved with internal boundary layer bleed(s) located on the compression ramp side and with a passive or an active shock boundary layer control device located on the cowl side. To design such a control system CFD and experiments will be used. On the experimental side detailed measurements are needed to provide a better understanding of the flow which will help in its modelisation. This is presently being done on a special test rig shown in figure 19a.

A supersonic nozzle delivers an upstream flow at a Mach number of 1.3/1.4 which is representative of the Mach number ahead of the last compression shock in the real air intake. The location of this shock can be adjusted with the throat located downstream. The test rig allows various geometries of the main boundary layer bleed to be tested and different shock control systems can be mounted on the upper side of the channel. Detailed flow field measurements can be performed with five holes probes and LDV. Figure 19 b shows an example of the flow field obtained with 2 independent suction areas through porous plates mounted on the opposite side of the main boundary layer bleed.

FIGURE 19 - Test set up for basic studies of air intakes

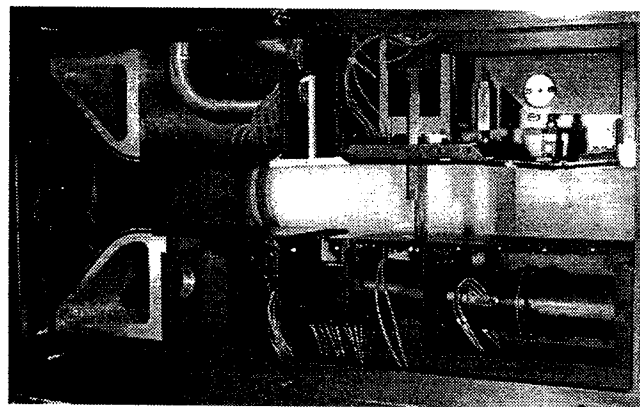


FIGURE 19a - Test rig

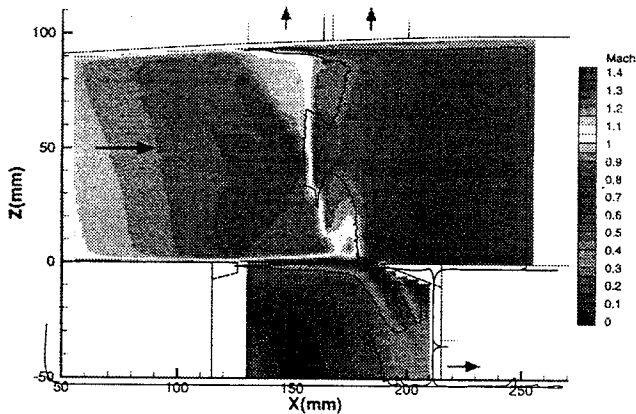


FIGURE 19b - Detailed flow measurement

Due to the great number of parameters to be investigated for the design of such a control system CFD will certainly be useful but unsteady, time accurate 3D Navier Stokes codes are needed. These codes are under development at ONERA and figure 20 presents an example of unsteady 2D Euler computations using the ALE technique <sup>(23)</sup> for the simulation of a quick change of the mass flow rate of a 2D air intake.

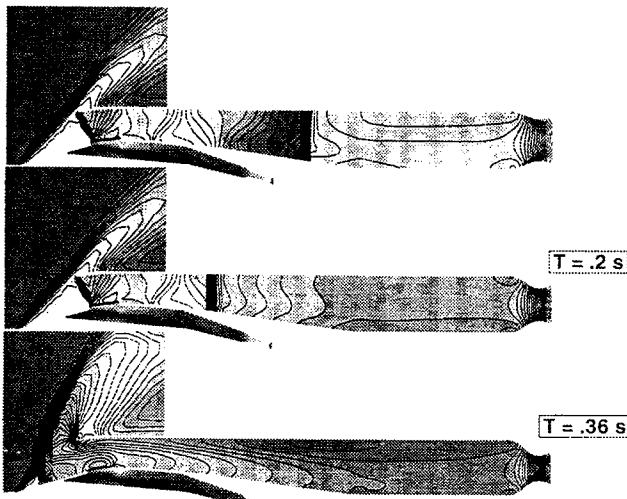


FIGURE 20 - Unsteady 2D Euler computations

Auxiliary air intakes

To improve the transonic cruise efficiency a bypass engine will probably be used for the future SCT aircraft but the bypass ratio will be small in order to reduce the engine diameter.

Thus, auxiliary air intakes will be used in order to increase the engine mass flow at subsonic speeds. The secondary flow passing through the fan will come both from the main air intake and from the auxiliary air intakes (figure 21).

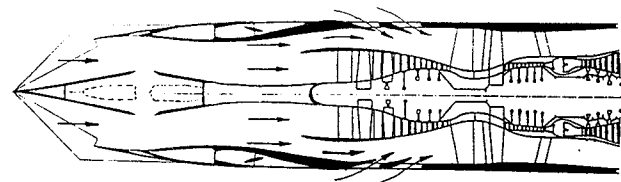


FIGURE 21 - Scheme of the MTF engine

In order to provide the fan with a flow having a high pressure recovery and low distortion, a careful design of the shape of these auxiliary air intakes is needed. This design has also to take into account geometrical constraints and has to be such that the nacelle drag is not increased too much. Figure 22 illustrates how CFD can help in the design of these air intakes. The figure compares flow fields computed in 2D with the Navier Stokes CANARI code on three different axisymmetric geometries (two flush inlets and a scoop inlet). The flush inlets have different curvature laws for the internal lip which generate more or less acceleration. The scoop inlet which exhibit a higher cross section allows to increase the fan mass flow compared to the flush inlets.

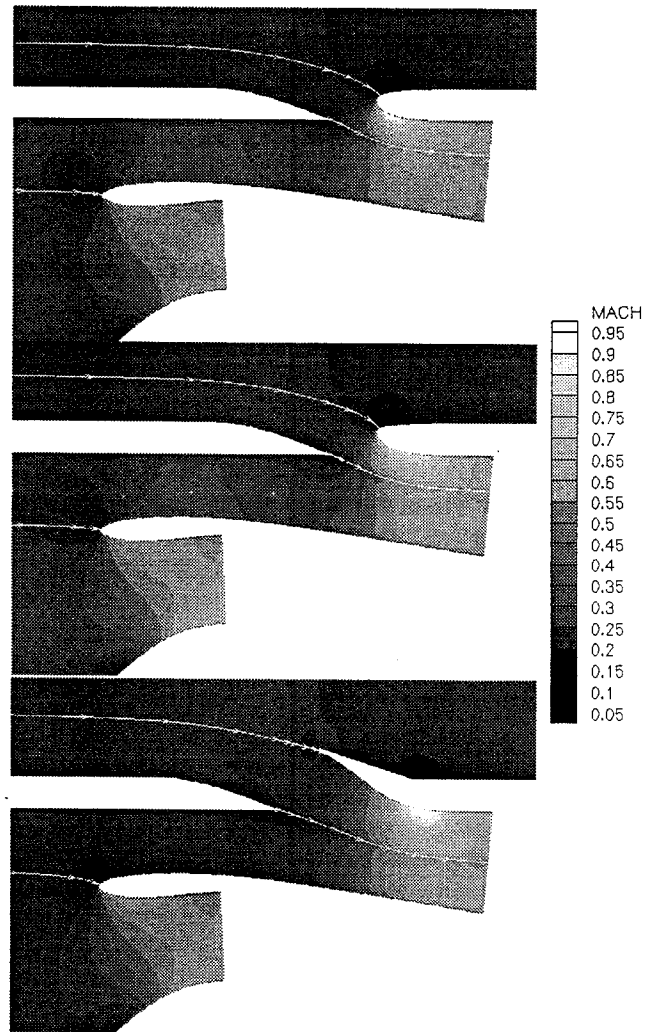


FIGURE 22 - Auxiliary air-intakes - Computed Flow field

### Conclusion

During these last few years ONERA activities on supersonic transport aircraft aerodynamics have been oriented towards CFD code assessment for performance prediction and in particular for the drag, the development of numerical optimisation tools for multipoint designs, drag reduction technology investigation and air intake aerodynamics.

From these studies the following conclusions can be drawn :

- Euler and Boundary Layer codes are able to predict the general feature of the flow around supersonic transport aircraft configurations for all the flight conditions. The accuracy concerning the drag prediction is quite satisfactory for supersonic cruise but not so for transonic cruise. At low speed and high angle of attack Euler codes exhibit too much artificial dissipation.
- The degree of accuracy needed for the prediction of the drag of this new aircraft needs further improvement of the Euler codes and the assessment of other codes like coupled codes and Navier Stokes codes.
- Numerical optimisation techniques have proven to be efficient for multipoints designs but they suffer from too large computing time and thus new algorithms have to be developed to reduce this computing time.
- Drag reduction technologies which have been extensively investigated for subsonic transport aircraft can also be used for supersonic aircraft. While riblets seems to be promising, laminar flow control provides small gains at least for the actual wing designs. Specific laminar designs are needed to evaluate the potential benefit but also to see if such designs are practical. Anyhow difficult technical problems will have to be solved for laminar flow control applications.
- CFD tools are able to predict correctly air intake performances near adaptation. They have still to prove their capacity for off design performance prediction as well as for shock control system designs which are needed for mixed compression air intakes.
- Comprehensive wind tunnel test are needed both for external and internal aerodynamic studies in order to get more confidence in using the CFD tools and also to better understand complex flow mechanisms.

- Flight testing would be of great value for improving wind tunnel to flight extrapolation methodology.

### References

- [1] - VUILLOT A.M., COUAILLER V., LIAMIS N.  
"3D turbomachinery Euler and Navier Stokes Calculations with a multidomain cell-centred approach".  
AIAA paper 93-2576, Monterey, 1993.
- [2] - LERAT A., SIDES J., DARU V.  
"An implicit finite volume method for solving the Euler equations."  
Lecture notes in Physics.  
Vol. 17, pp 343-349, 1982
- [3] - JAMESON A., SCHMIDT W., TURKEL E.  
"Numerical solution of the Euler equations by finite volume methods."  
AIAA paper 81-1259, 1981
- [4] - HOUEVILLE R.  
"Three-dimensional boundary layer calculation by a characteristic method using Runge-Kutta time stepping schemes."  
5<sup>th</sup> Symposium on Numerical and Physical Aspects of Aerodynamic Flows, Long Beach, January 1992.
- [5] - COUSTOLS E. and ARNAL D.  
"Skin friction Prediction and reduction".  
International CFD Workshop for Supersonic Transport Design, Tokyo, March 1998.
- [6] - THIBERT J.J.  
"One point and multi-point design optimisation for airplane and helicopter application."  
AGARD FDP/VKI Special course on Inverse Methods for Airfoil Design for Aeronautical and Turbomachinery Applications. AGARD report n° 780 paper n° 10.
- [7] - DESTARAC D., RENEUX J.  
"Applications de l'optimisation numérique à l'aérodynamique des avions de Transport."  
La Recherche Aérospatiale, 1993 n° 2 p. 39-55
- [8] - VANDERPLAATS Garret N.  
"CONMIN- A fortran Program for Constrained Function Minimization".  
NASATMX 62, 282 - August 1973.

- [9] - VANDERPLAATS Garret N.  
"COPEs - A Fortran Control Program for Engineering Synthesis."
- [10] - GRENON R.  
"Numerical Optimization in Aerodynamic Design with application to a Supersonic Transport Aircraft".  
NAL International Workshop on Supersonic Transport Design, Tokyo, March 1998
- [11] - RENEAUX J., THIBERT J.J., SCHMITT V.  
"ONERA activities on drag reduction"  
ICAS paper 90-3.6.1
- [12] - SCHMITT V., HINSINGER R.  
"Advanced transport aircraft aerodynamics in cooperation with Airbus Industrie".  
La Recherche Aérospatiale, 1996, n° 4, p. 265-277.
- [13] - COUSTOLS E., SCHMITT V.  
"Synthesis of experimental Riblet studies in transonic conditions in Turbulence Control by passive means"  
COUSTOLS E. Ed, Klumer Academic Publisher, 1990
- [14] - COUSTOLS E. and COUSTEIX J.  
"Performances of riblets in the Supersonic regime"  
AIAA JOURNAL, VOL 32, n° 2. Technical notes.
- [15] - ARNAL D.  
"Transition prediction in transonic flow"  
IUTAM Symposium Transsonicum III. DFVLR - AVA Göttingen 1988.
- [16] - COUSTOLS E.  
"Stabilité et transition en écoulement tridimensionnel : cas des ailes en flèche."  
Thèse de Docteur-Ingénieur ENSAE (Juin 1983).
- [17] - ARNAL D.  
"Boundary layer Transition predictions based on Linear Theory."  
AGARD FDP/VKI Special Course on Progress in Transition Modelling - AGARD Report n° 793.
- [18] - RENEAUX J., PREIST J., JUILLEN J.C., ARNAL D.  
"Control of attachment line contamination."  
2<sup>nd</sup> European Forum on Laminar Flow Technology.  
Bordeaux (France), June 10, 1996 - ONERA TP 1996-84
- [19] - ARNAL D.  
"Etude des possibilités de réduction de Traînée par laminarisation."  
7<sup>th</sup> European Aerospace Conference EAC 94 Toulouse, October 1994.
- [20] - LEYNAERT J.  
"Transport Aircraft intake design"  
VKI - Lecture series 1988-04 Intake aerodynamics - ONERA TP 1988-18
- [21] - LEYNAERT J.  
"Les prises d'air et arrière-corps de moteur des avions subsoniques et supersoniques. Eléments généraux."  
25<sup>e</sup> colloque d'Aérodynamique Appliquée, Talence, October 1988 ONERA TP 1988-132.
- [22] - CAMBIER L., DARACQ D., GAZAIX M., GUILLEN Ph., JOUET Ch., LE TOULLEC L.  
"Améliorations récentes du code de calcul d'écoulement compressible FLU3M."  
AGARD Séville, Espagne 2-5 Octobre 1995.
- [23] - THIERRY G.  
"Simulations d'écoulements de fluides parfaits autour de corps déformables. Applications à l'aéroélasticité des lanceurs."  
Thèse de doctorat de l'Université de Paris Nord, 1998.